

Title	Simultaneous optical second harmonic and sum frequency intensity image observation of hydrogen deficiency on a H-Si(1 1 1) 1 × 1 surface after IR light pulse irradiation
Author(s)	Miyauchi, Y.; Sano, H.; Okada, J.; Yamashita, H.; Mizutani, G.
Citation	Surface Science, 603(19): 2972-2977
Issue Date	2009-10-01
Type	Journal Article
Text version	author
URL	http://hdl.handle.net/10119/9050
Rights	NOTICE: This is the author's version of a work accepted for publication by Elsevier. Y. Miyauchi, H. Sano, J. Okada, H. Yamashita, and G. Mizutani, Surface Science, 603(19), 2009, 2972-2977, http://dx.doi.org/10.1016/j.susc.2009.08.003
Description	

Simultaneous optical second harmonic and sum frequency intensity image observation of hydrogen deficiency on a H-Si(111) 1×1 surface after IR light pulse irradiation

Y. Miyauchi^{1, 2}, H. Sano^{1, 2, 3}, J. Okada¹, H. Yamashita¹, and G. Mizutani^{1, 2}

¹School of Materials Science, Japan Advanced Institute of Science and Technology,
1-1 Asahidai, Nomi, Ishikawa 923-1292, JAPAN

²Japan Science and Technology Agency – Core Research for Evolutional Science and
Technology, 5-3 Sanban-cho, Chiyoda-ku, Tokyo

³Ishikawa National College of Technology,
Kitachujo, Tsubata, Kahoku-gun, Ishikawa, 929-0392 JAPAN

Abstract

In this study, we have developed a microscope for simultaneous acquisition of optical sum frequency (SF) and second harmonic (SH) intensity images in UHV conditions, and observed resonant electronic and vibrational images of the H-Si(111) surface after IR light irradiation of pulse width ~6μs. The SH intensity images showed a spatial distribution of resonant electronic states, associated with dangling bonds formed after hydrogen desorption induced by the IR light pulses. This result indicates that the hydrogen coverage decreased to less than ~0.6ML in the irradiated area. The SF intensity images before the IR light pulse irradiation showed signals attributed to the Si-H stretching vibration on the H-Si(111) surface. After the IR light pulse irradiation, non-resonant SF signals appeared in the irradiated area. The non-resonant SF signals may originate from a nonlinear optical transition involving the surface electronic levels in the dangling bonds. We also found an unidentified bonding state on the edges of the irradiated area in some light conditions. Both the resonant and non-resonant signals were very weak in this area.

Keyword

Sum frequency generation, Second harmonic generation, Sum frequency microscopy, Second harmonic microscopy, Laser induced thermal desorption, Silicon, Hydrides

Introduction

The hydrogen desorption promoted by rapid temperature rise on a Si surface after light pulse irradiation is known as laser induced thermal desorption (LITD). The LITD process is utilized in the optical chemical vapor deposition (CVD) growth technique and has been studied well [1,2]. In the practical optical CVD growth of a uniform Si film, spatial uniformity of coverage and the orientation of H-Si bonds are important. However, in the LITD process the spatial distribution changes dramatically as a function of the power density, the wavelength, and the duration of the incident light pulse, because LITD is an indirect process promoted by the rapid temperature rise after incident light pulse irradiation [1,3]. One also has to consider the effect of electron-hole plasma excitation on the hydrogen desorption [1].

For the application of the LITD process, it is important to investigate the spatial distribution of the coverage and the orientation of the Si-H bonds on the Si surface after pulse light irradiation [4,5,6]. However, there have been only a small number of reports on the spatial distribution of hydrogen coverage on a Si surface [3,6,7]. Concerning the spatial distribution of the orientation and vibrational mode of the Si-H bonds, there have been no reports. One of the reasons for the difficulty in determining the chemical bonding state during the LITD process may be the lack of techniques for monitoring a two-dimensional distribution image of hydrogen on a Si surface.

In order to establish a technique for such observation, we have developed a visible-IR sum frequency microscope operating in ultra high vacuum (UHV) conditions. The SF microscopy will enable us to observe a resonant vibrational image on a Si(111) surface. It is expected to be useful for detecting the spatial variation of the orientation and the vibrational mode of the Si-H bonds. The peak wavenumber of the SF response reflects the species of the hydrides. We have further added the function of detecting optical second harmonic generation (SHG) and have built up a system for observing SF and SH images simultaneously.

SFG and SHG are the lowest-order nonlinear optical processes. They occur in media without inversion symmetry and have high surface sensitivity [8]. SHG has been used as a tool to investigate the surface structures [9] and surface electronic states associated with dangling bonds on a Si surface. It was used to estimate the speed of hydrogen adsorption [10] and the diffusion constant of hydrogen [11] on a Si(111) surface. Recently, it has been applied to microscopy [12] for monitoring the spatial distribution of dangling bonds on a Si(111) surface [3,6].

SFG is a useful tool for studying Si-H bonds [13] and identifying hydride species [14] on a Si surface. In order to analyze the non-uniform reaction of hydrogen on a Si surface with complicated spatial structures – to be used, e.g., in integrated circuits during fabrication – it is necessary to observe the two-dimensional distribution of vibration in hydrides. This is difficult to do with conventional vibrational microscopy, such as Raman and IR microscopy, because these techniques

are not sufficiently sensitive. Thus it will be advantageous to employ SFG in microscopy. By observing the contrasts in both the SF and SH intensity images, one will distinguish clearly between the H-Si(111) surface areas irradiated and not irradiated by the light pulses.

By simultaneous SF and SH microscopy, one can evaluate the coverage, the orientation and the vibrational mode of Si-H bonds more systematically than by separate observations. As a demonstration of this system, we observed hydrogen deficiency of a H-Si(111) surface irradiated by IR light pulses with the temporal width of $\sim 6\mu\text{s}$ (Hereafter we call this light pulse a *desorption-inducer* IR light pulse). The hydrogen desorption process promoted by the desorption-inducer IR light pulse in this study is a LTD process, as we have confirmed by LTD model simulation (not shown).

In the SH intensity images obtained in this study, we have first confirmed that dangling bonds were formed after hydrogen desorption in the area irradiated by the desorption-inducer IR light pulses. Then, in the SF intensity images, non-resonant signals were observed in the irradiated area. We also found that a boundary area occurs between the areas with resonant and non-resonant SF signals in some irradiation light conditions. Neither resonant nor non-resonant signals are observed in this boundary area. This last result suggests the occurrence of a special Si-H bonding state at the edge of the focused light spot on the surface. It can be observed only by SF microscopy.

Experimental

The system for observing simultaneous SF and SH intensity images in UHV conditions is shown in Fig. 1. In the SF microscopy system, we used doubled frequency output from a mode-locked Nd³⁺:YAG laser as the visible light at wavelength 532nm, and output ($\sim 4.8\mu\text{m}$) from an optical parametric generator and amplifier system (OPG/OPA) as the wavelength-tunable infrared light (IR probe light). The spectral bandwidth of the IR probe light was 6 cm^{-1} . The pulse energies of the IR probe and visible light beams were $\sim 100\mu\text{J/pulse}$ and $\sim 25\mu\text{J/pulse}$, respectively.

The incident visible light was passed through a $\lambda/2$ plate, a Glan polarizer, a bandpass filter with center wavelength of 532nm, a lens with focal length $f=300\text{mm}$, and the CaF₂ window of the UHV chamber. The IR probe light was focused by a CaF₂ lens with focal length of 300mm. The angles of the incident visible and IR probe light beams were $\sim 45^\circ$ and $\sim 60^\circ$, respectively.

The SF light from the sample in the reflective direction was first passed through the glass window of the chamber and dichroic filters to block the incident visible light, and was then introduced into a long-distance Cassegrain-type microscope (Quester QM-1). The microscope was equipped with a time-gated image-intensified charge-coupled device (CCD) camera (Hamamatsu PMA-100-H) for accumulating the SF and SH signals. With this long-distance microscope, the image of an object 0.5m away can be focused on the detector plane with a resolution of $\sim 3\mu\text{m}$. The microscope was also equipped with band-pass filters with center wavelengths of 490nm for SF microscopy and 532nm for SH microscopy. The polarizations of the SF, visible, and IR light were all, p, and p, respectively. For SF spectroscopy, the SF light was passed through a double monochromator, and detected by a photo-multiplier and a gated integrator. The excitation light for SHG (with a wavelength of 1064nm and power of $\sim 40\mu\text{J/pulse}$) was generated by the same OPG/OPA system as that used in the SFG measurement. The polarizations of the incident light and the SH light were p and all, respectively. The integration time for taking SF and SH intensity images was 500 seconds each. It was confirmed that luminescence signals under these measurement conditions were very weak.

We paid special attention to the following points in the development of the SF and SH microscopy system. Our previous SH microscope had a problem, in that the images were modified by the non-uniform intensity distribution in the beam pattern of the incident light [3]. In order to avoid this modification, we moved the irradiating position on the sample in the raster scan by moving the focusing lenses using an automatic X-Y stage. It is difficult to take the SF and SH microscopic images in exactly the same condition, since the incident light beams from different sources must be focused on the same area on the sample surface. In order to make the spot positions of the incident light beams exactly the same, we switched the optical paths of the incident light for SH microscopy and that of the incident visible light for SF microscopy using a prism beam

exchange mechanism. By these innovations, we succeeded in taking simultaneous SF and SH intensity images.

To prepare a H-Si(111)1×1 surface, n-type Si(111) wafers with resistivity $\rho=200\sim240\ \Omega\text{cm}$ were etched in a clean room by a few cycles of dipping in a hot solution of 97% H_2SO_4 : 30% H_2O_2 = 4:1, then in hydrofluoric acid, and finally in NH_4F solutions to produce monohydride terminated Si(111) surfaces [15]. After this treatment, the sample was immediately introduced into the UHV chamber. We have confirmed a 1×1 structure of the H-Si(111) surface thus prepared, through a low energy electron diffraction (LEED) measurement.

In order to promote hydrogen desorption, the Si surface was irradiated with *desorption-inducer* IR light pulses (Wavelength: 1064nm, Pulse duration: $\sim 6\mu\text{s}$, Repetition rate: 10Hz, Pulse energy: 6~12mJ/pulse, Focus size: $\sim 0.1\text{mm}$, total irradiation time for drawing a circle pattern: $\sim 32\text{s}$, irradiating time/one point: $\sim 2\text{s}$) from a Nd^{3+} : YAG laser. When we irradiated the *desorption-inducer* IR light pulses, we moved the lenses in front of the sample using an automatic X-Y stage, and scanned the focusing spot over the Si surface in a circular pattern. We confirmed that there was no melting or damage on the Si surface by taking a linear microphotograph.

Results and discussion

We irradiated the H-Si(111) 1×1 surface with the desorption-inducer IR light pulses, drawing a circle of a diameter of $\sim 0.2\text{mm}$ and a dot at the center of the circle, and observed the SF and SH intensity images. Fig. 2(a) shows a SH intensity image of the H-Si(111) surface soon after the irradiation by the desorption-inducer IR light pulses. The bright dots represent SH photons, and the scale bar corresponds to $200\mu\text{m}$. The SH signals are observed at the irradiated area in a circular shape with diameter of $\sim 0.2\text{mm}$ and in a dotted shape at the center of the circle.

This result is interpreted as follows. The desorption-inducer IR light gave rise to hydrogen desorption from the H-Si(111) surface and generated many dangling bonds. Since surface electronic levels due to the dangling bonds are formed around the Fermi level on the energy axis, a resonant optical transition mediated by these surface electronic levels occurred at the incident photon energy $\hbar\omega=1.17\text{eV}$ and enhanced the SHG [11,16]. On the other hand, the H-terminated surface has no surface state in the energy band gap, and SHG enhancement due to resonant optical transition did not occur at $\hbar\omega=1.17\text{eV}$.

It is useful to note that the SH signals are also sensitive to surface melting. In our previous paper, we reported that enhanced SH light was generated in an area irradiated by UV light pulses on a Si(111) surface, due not only to dangling bonds, but also to surface melting [3]. The SH light from the molten surface did not disappear after the exposure of the surface to air of 1 atm. In order to determine the origin of the SH signals shown in Fig. 2(a), we checked if the SH signals disappeared after a hydrogen exposure of ~ 3 Torr for 5 minutes. Since the probability of hydrogen adsorption is very low [11], the impurities in the UHV chamber (e.g., CO, CO₂ and H₂O molecules) were mainly adsorbed on the Si surface when hydrogen molecules were introduced. As a result, the SH signal completely disappeared (not shown). This result indicates that the enhanced SH light was caused by dangling bond formation on the Si surface. It also shows that the surface did not melt due to the IR light pulse irradiation.

We note here that the hydrogen coverage on our surfaces could not be estimated from our SHG observation. The SH signals from the Si(111) surface are known to be sensitive to hydrogen coverage only at low coverages, less than 0.6ML [11,17]. However, in order to estimate the lower coverages, SH intensity from a clean Si surface is also necessary. In our experimental conditions we could not obtain the SH intensity from a clean Si surface, so we could obtain only relative coverages. We can only say that the coverage of hydrogen in the area emitting the enhanced SH signals is less than $\sim 0.6\text{ML}$.

Figure 2(b) shows a SF intensity image of the irradiated H-Si(111) surface with the IR probe wavenumber of 2080cm^{-1} resonant with the Si-H stretching vibrational mode. The area not irradiated by the desorption-inducer IR light pulse was terminated by monohydride, and thus shows

resonant SF signals. The areas irradiated by the desorption-inducer IR light pulses in circular and dotted shapes show stronger SF response. Fig. 2(c) shows a SF intensity image with the IR probe light wavenumber of 2060 cm^{-1} off-resonant with any Si-H vibrational mode. We see no SF signals in the area not irradiated by the desorption-inducer IR light pulses. However, enhanced SF signals are seen in the irradiated area in Fig. 2(c) at similar intensity to those in Fig. 2(a) and (b). From Figs. 2(b) and (c), the SF signals in the irradiated area do not appear to be resonant with the vibration of Si-H bonds.

In order to investigate the origin of the SF signals in the irradiated area, we have measured the SF spectrum of a H-Si(111) surface after desorption-inducer IR light pulse irradiation. The desorption-inducer IR light pulses irradiated an area of $\sim 2\text{ mm}^2$ on the Si surface, and then the SF spectrum of the area was measured. We carefully confirmed that the spots of the IR probe light and the visible light were within the irradiated area on the Si surface. We also measured the SF intensity spectrum of the reference GaAs and the H-Si(111) surface, and then normalized the latter by the former.

Figure 3 shows the SF intensity spectra of the H-Si(111) surface prepared in the way stated above. The black squares, gray triangles, light grey circles represent the SF intensity of a H-Si(111) surface before, 10 minutes after, and 18 hours after the irradiation by the desorption-inducer IR light pulses, respectively. The estimated exposure of impurity gas in 18 hours is $\sim 27\text{ L}$. The sharp peak at 2080 cm^{-1} in the spectrum of the Si surface before irradiation is attributed to the stretching vibration of the monohydride species. We note that Higashi and his coworkers performed an ATR-IR measurement of a H-Si(111) surface (with the resolution of $\sim 0.5\text{ cm}^{-1}$), and assigned the peak at 2083.7 cm^{-1} as being due to the Si-H stretching vibration [15]. The probe light in our work has bandwidth of $\sim 6\text{ cm}^{-1}$, so we cannot measure a peak with a better resolution than $\sim 6\text{ cm}^{-1}$. Within this spectral resolution the peak observed at 2080 cm^{-1} in this work should be assigned as being due to the same Si-H stretching vibration as that observed by Higashi et al.

In the SF spectrum of the surface 10 minutes after the irradiation, the peak at 2080 cm^{-1} disappeared and the SF signal intensity was almost constant from 2060 to 2140 cm^{-1} . This result indicates that the SF signals in the irradiated area did not occur due to resonance with any vibrational mode. In the SF spectrum of the surface 18 hours after irradiation, the signal is uniformly weaker and has no peak (light grey circles in Fig. 3). However, the SF spectrum in the non-irradiated area did not change significantly even after 18 hours. Thus, the decrease of the non-resonant SF signals in the irradiated area is due to the adsorption of the impurity gas in the UHV chamber. 90% of the SF signals from the irradiated area disappeared after the exposure to air of 1 atm in another experiment. These results suggest that most of the SF signals in the irradiated area are due to a surface electronic level associated with the dangling bonds formed after hydrogen desorption.

Sano and his coworkers calculated the nonlinear susceptibility of a Si(111) 1×1 surface by a first principle density functional method for analyzing the SH signals from the surface [16]. We use their results in order to discuss the origin of the observed non-resonant SF signals from the irradiated H-Si(111) surface. Here both SHG and SFG are three photon processes, but are different in that the two incident photon energies are the same in the former and different in the latter. Thus, the mechanism of the NR-SF signal enhancement due to the optical transition to the intermediate state may be similar to that of SH signal enhancement. Thus, it is reasonable to compare the non-resonant SF signals with the calculated susceptibility of SHG.

Hereafter we call the SF signals attributed to the Si-H vibrational mode “RV (Resonant Vibrational)–SF signals” and SF signals from the H-Si(111) surface irradiated by desorption-inducer IR light pulses “NR (Non-Resonant)-SF signals”. Sano and his coworkers calculated the nonlinear susceptibility $\chi^{(2)}$ of the H-Si(111) 1×1 and Si(111) 1×1 surfaces. We do not know experimentally whether the structure of the H-Si(111) surface after irradiation by the desorption-inducer IR light pulses was an ideal 1×1 or 7×7 structure, since roughening might have occurred on the surface irradiated by the strong light pulses. We tried to observe a LEED pattern of the Si surface after IR light pulse irradiation in order to investigate the surface structure, but could not observe any change from 1×1 pattern. This is probably because the observed area was wider than the irradiated area. Nevertheless, in our present analysis, in order to get an insight into the origin of the NR-SF signals, we assumed the surface to be a 1×1 surface, since there is no available calculation about the 7×7 surface so far as we know.

As a possible origin, the NR-SF signals may have been enhanced due to optical transition by the visible probe light with photon energy of $\sim 2.34\text{eV}$. However, according to Sano and his coworkers, the value of the $\chi^{(2)}$ components of Si(111) 1×1 and H-Si(111) 1×1 are not significantly different from each other at $\sim 2.34\text{eV}$. Since the signals disappeared due to the hydrogen termination, the NR-SF signals were not resonantly enhanced due to the optical transition to the surface electronic level by the incident visible light.

As another candidate origin, the signals may have been enhanced due to electronic transition by the IR probe light. We discuss the second-order nonlinear susceptibility $\chi^{(2)}$ for the incident photon energy below 1eV , since the photon energy of the incident IR probe light in the present study is $\sim 0.26\text{eV}$. In fact there has been no experimental report on a linear reflection spectrum below $\sim 0.5\text{eV}$, so we again refer to the result by Sano and his coworkers [16]. According to Sano and his coworkers, all active $\chi^{(2)}$ components of the H-Si(111) 1×1 surface should be zero for incident photon energy below 1eV . On the other hand, components of a Si(111) 1×1 surface have two peaks at $\hbar\omega \sim 1.25\text{eV}$ and $\sim 0.5\text{eV}$. Sano and his coworkers attributed the peak around $\sim 0.5\text{eV}$ to the electronic transition from the valence band to the surface electronic levels associated with the dangling bonds[16]. The calculated peak around $\sim 0.5\text{eV}$ is broad, and the peaks of all active $\chi^{(2)}$

components have their tails to $\sim 0.2\text{eV}$. Thus the NR-SF signals might well be enhanced due to the optical transition to the surface electronic state, excited off-resonantly by the IR probe light with photon energy of 0.26eV . In order to assign the NR-SF signals accurately, the SF spectrum of a spectral range much broader than the present study is required.

In order to monitor the change of the distribution of the SF signals with time after irradiation by the desorption-inducer IR light pulses, we took SF intensity images 10 minutes and 22 hours after the irradiation. P-polarized desorption-inducer IR light pulses of the power of 14, 15, 16 mJ/pulse irradiated the surface, in circular pattern with diameters of 0.6, 0.35, 0.1mm, respectively. The exposure of the surface to impurities during 22 hours was $\sim 30\text{L}$. From a linear microphotograph image, we found that a small part of the area irradiated by the pulses at 16 mJ/pulse was damaged.

Figures 4(a) and (b) show the SF intensity images of the H-Si(111) surface with the IR probe light wavenumber of 2080cm^{-1} 10 minutes and 22 hours after irradiation by the desorption-inducer IR light pulses, respectively. In Fig. 4(a), RV-SF signals are seen in the non-irradiated area, and NR-SF signals are seen in the irradiated area. In Fig. 4(b), the intensity of the RV-SF signals did not decrease remarkably, but the NR-SF signals were reduced, and thus the irradiated area looks darker.

Figures 4(c) and (d) show the SF intensity images of the Si surface with the IR probe light wavenumber of 1950cm^{-1} 10 minutes and 22 hours after the IR light pulse irradiation, respectively. In Fig. 4(d), the NR-SF signals are much weaker than those in Fig. 4(c). The reductions of the NR-SF signals seen from Fig. 4(a) to (b) and from (c) to (d) show the same tendency as those of the SF intensity spectrum in Fig. 3 in the irradiated area after 18 hours.

In Fig. 4(a), we see a boundary between the areas with intense RV-SF and NR-SF signals after IR light pulse irradiation at the power of 14mJ/pulse, as shown by an arrow. There are two candidate origins of the occurrence of this boundary area.

- (1) The SF signals disappeared at the boundary area due to negative interference of the RV-SF and NR-SF signals [18].
- (2) At the boundary area, the orientation of the Si-H bonds was disordered, or the desorption of hydrogen did not leave enough dangling bonds, and neither RV-SF nor NR-SF signals were strong.

The candidate (1) is denied for the following reason. If the dark boundary area in Fig. 4(a) occurred due to the negative interference of the RV-SF and NR-SF signals, the former should dominate the boundary area when the latter are reduced. Then, the width of the dark area in Fig. 4(b) showed to be narrower than the total width of the area with the NR-SF signals and the boundary in Fig. 4(a). However, the widths of the areas shown in Fig. 4(a) and (b) are estimated as $51.8\mu\text{m}$ and $56.5\mu\text{m}$ respectively. The width in Fig. 4(b) did not become narrower than the width in Fig. 4(a). Thus, candidate (1) is not feasible as the origin of the boundary area formation.

We note that the dark area widths were estimated from the SF intensity profile in the direction

perpendicular to the dark line. We fitted Gaussian distributions to the falling edges of the RV-SF signals and the rising edges of the NR-SF signals, and used the full width of half maximum (FWHM) of the Gaussian distributions to estimate the widths.

In the candidate origin (2), reduction of NR-SF signals in the boundary area may be due to low density of the surface dangling bonds. In order to investigate the spatial distribution of the hydrogen coverage in the boundary area, a SH intensity image was observed 22 hours after irradiation by desorption-inducer IR light pulse irradiation, as it is shown in Fig. 4(e). Since the enhanced SH signals due to the dangling bonds are seen in Fig. 4(e), the absorption of the impurities in the irradiated area is judged to be still below 0.6ML after 22 hours. The width of the area emitting SH signals in Fig. 4(e) is estimated to be $34.7\mu\text{m}$. This width is less than that of the dark area in RV-SF signals ($51.8\mu\text{m}$) in Fig. 4(b), and is close to that of the area of NR-SF signals ($38.2\mu\text{m}$) in Fig. 4(a). Consequently, in the boundary area, the coverage of hydrogen is larger than 0.6ML. Thus, the reason for the weak NR-SF signals at the boundary area may be considered to be the low density of the surface dangling bonds.

According to candidate origin (2), reduction of RV-SF signals in the boundary area originates from the reduction of hydrogen coverage, or from the disordering of the orientation of the H-Si bonds. By strong IR light irradiation, not only hydrogen desorption but also the disorder of Si-H bond orientation might occur on the Si surface. Even if the Si(111) surface is terminated by hydrogen with coverage of 1ML, RV-SF signals may not be generated efficiently due to the disordering of the orientation of Si-H bonds [14]. Since it was not possible to determine the microscopic structure of the irradiated Si surface, we could not confirm which candidate in the origin (2) was dominant in the reduction of the RV-SF signals at the boundary area. In order to find the details of the bonding state of the surface in the boundary area, further studies are necessary.

In Fig. 4(a), we notice that dark boundary areas of SF signals do not appear clearly for the inner two circles. This may be because the LITD process of hydrogen occurred throughout the whole irradiated area due to the higher intensity of desorption-inducer IR light pulses, and the density of the dangling bonds of the entire irradiated area became high enough for NR-SF signal generation.

We suggest that the change of the hydrogen coverage or the orientation of the Si-H bonds dynamically affects the properties of the epitaxial Si layer during the CVD growth. Thus, the new bonding state found in this study may increase knowledge of the hydride change in optical CVD growth, and it may lead to the development of new devices, such as solar cells with improved light-induced degradation properties. The present study demonstrates that the SF and SH microscopes are useful tools for observing the light pulse modification of a H-Si(111) surface.

Conclusion

In this study, we have developed a microscope for simultaneous observation of SF and SH images, and have observed a H-Si(111) surface after irradiation by desorption-inducer IR light pulses. We have obtained the first SF images of a solid surface in an ultra high vacuum condition. We have found that after irradiation by the desorption-inducer IR light pulses, the SH signals were enhanced due to dangling bonds formation after hydrogen desorption. Non-resonant SF signals appeared after irradiation by desorption-inducer IR light pulses. By observing the spatial distribution of resonant and non-resonant SF signals, we have found an unidentified bonding state on the edges of the irradiated area in some light conditions. Both the resonant and non-resonant signals were very weak in this area.

Reference

- [1] B. G. Koehler, and S. M. George, *Surf. Sci.* **248**, 158 (1991).
- [2] V. Yu. Timoshenko, Th. Dittrich, F. Koch, B. V. Kamenev, and J. Rapich, *Appl. Phys. Lett.* **77**, 3006 (2000).
- [3] Y. Miyauchi, H. Sano, and G. Mizutani, *e-J. Surf. Sci. Nanotech.* **4**, 105 (2006).
- [4] B. G. Koehler, C. H. Mak, D. A. Arthur, P. A. Coon, S. M. George, *J. Chem. Phys.* **89**, 1709 (1988).
- [5] M. L. Wise, B. G. Koehler, P. Gupta, P. A. Coon, and S. M. George, *Surf. Sci.* **258**, 166 (1991).
- [6] Y. Miyauchi, H. Sano, and G. Mizutani, *Appl. Surf. Sci.* **255**, 3442 (2008).
- [7] K. Ishikawa, K. Ueda, and M. Yoshimura, *Surf. Sci.* **433-435** 244 (1999).
- [8] Y. R. Shen, *The Principles of Nonlinear Optics* (Wiley, New York, 1984), pp. 84.
- [9] T. F. Heinz, M. M. T. Loy, and W. A. Thompson, *Phys. Rev. Lett.* **54**, 63 (1985).
- [10] P. Bratu, and U. Höfer, *Phys. Rev. Lett.* **74**, 1625 (1995).
- [11] G. A. Reider, U. Höfer, and T. F. Heinz, *Phys. Rev. Lett.* **66**, 1994 (1991).
- [12] Y. Sonoda, G. Mizutani, H. Sano, S. Ushioda, T. Seikya, and S. Kurita, *Jpn. J. Appl. Phys.* **39**, L253 (2000).
- [13] P. Guyot-Sionnest, *Phys. Rev. Lett.* **66**, 1489 (1991).
- [14] M. Y. Mao, P. B. Miranda, D. S. Kim, and Y. R. Shen, *Appl. Phys. Lett.* **75**, 3357 (1999).
- [15] G. S. Higashi, Y. J. Chabal, G. W. Trucks, and K. Raghavachari, *Appl. Phys. Lett.* **56**, 656 (1990).
- [16] H. Sano, G. Mizutani, W. Wolf, and R. Podloucky, *Phys. Rev. B* **66**, 195338 (2002).
- [17] G. A. Reider, U. Höfer, and T. F. Heinz, *J. Chem. Phys.* **94**, 4080 (1991).
- [18] M. Himmelhaus, F. Eisert, M. Buck, and M. Grunze, *J. Phys. Chem. B* **104**, 576 (2000).

Figure caption

Fig. 1. Optical setup of the SF and SH microscopy.

Fig. 2. (a) SH intensity image of H-Si(111)1×1 surfaces after desorption-inducer IR light pulse irradiation, and (b) and (c) SF intensity images of the same surface with IR probe light wavenumber of 2080cm^{-1} and 2060cm^{-1} , respectively. The bright dots represent the observed SH or SF photons. The scale bars represent $200\mu\text{m}$.

Fig. 3. SF intensity spectrum of the H-Si(111)1×1 surface before (black squares), 10 minutes after (dark gray triangles), and 18 hours after (light grey circles) IR light pulse irradiation

Fig. 4. SF and SH intensity images of H-Si(111) surface after irradiation by the desorption-inducer IR light pulses. (a) SF intensity image 10 minutes after pulse irradiation [2080cm^{-1}] (the white arrow shows the dark boundary area between the areas with resonant and non-resonant SF signals), (b) SF intensity image 22 hours after pulse irradiation [2080cm^{-1}], (c) SF intensity image 10 minutes after pulse irradiation [1950cm^{-1}], (d) SF intensity image 22 hours after the pulse irradiation [1950cm^{-1}], and (e) SH intensity image 22 hours after pulse irradiation [$2\hbar\omega=2.33\text{eV}$]. The bright dots represent the observed SF or SH photons. . The scale bars represent $200\mu\text{m}$.

Figures

Figure 1

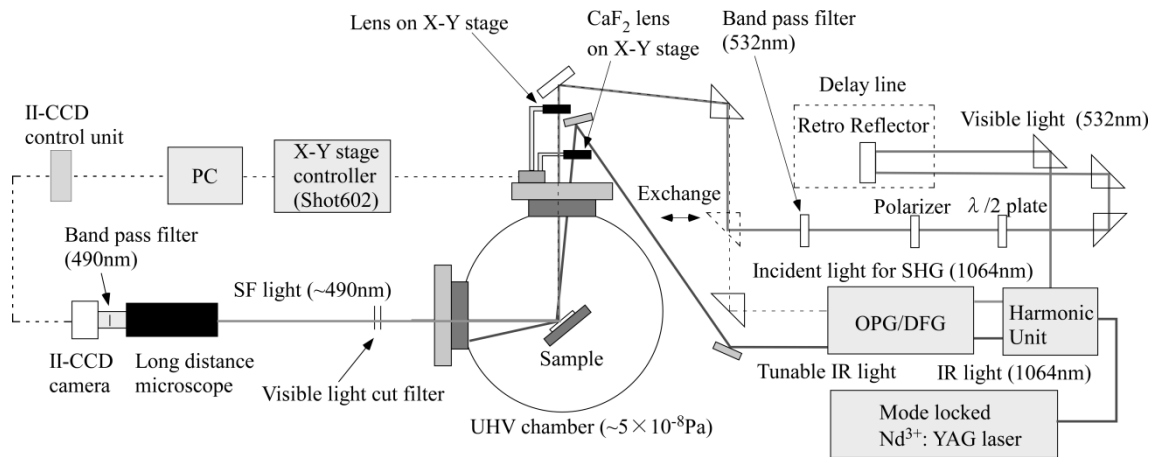


Figure 2

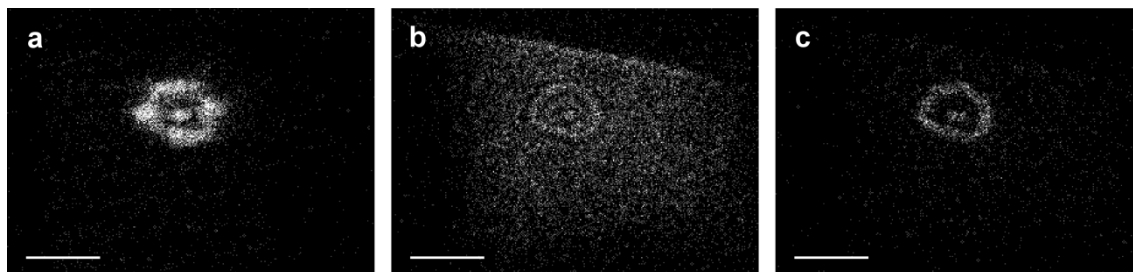
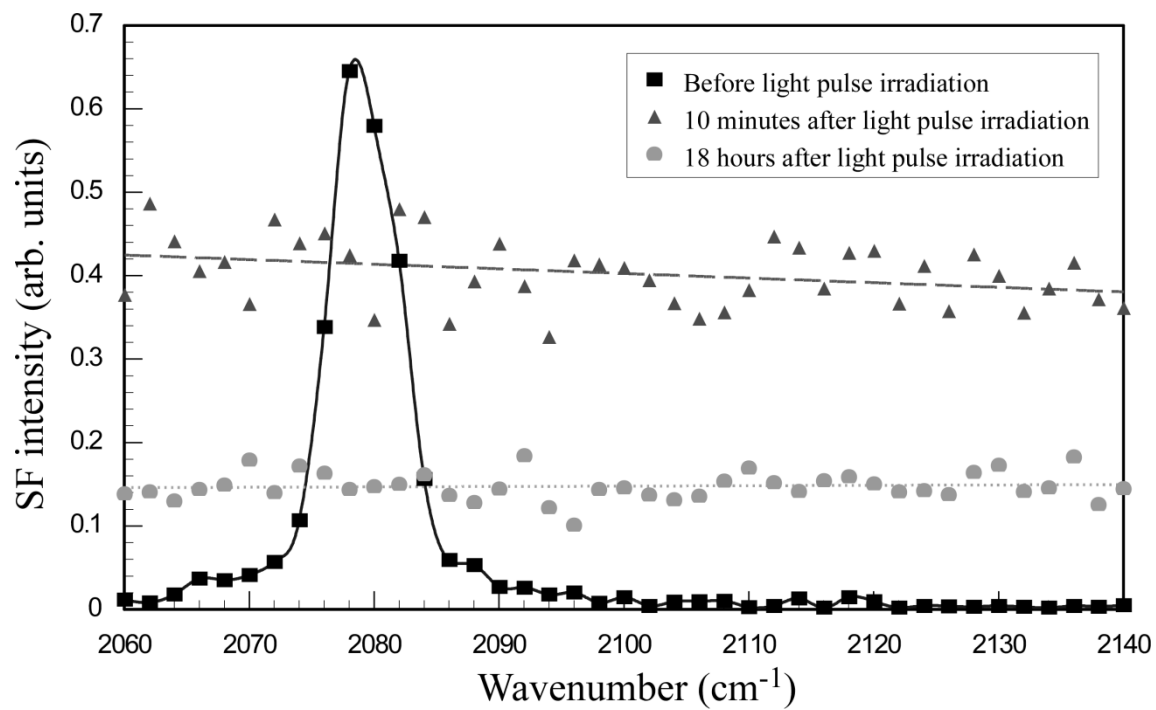


Figure 3



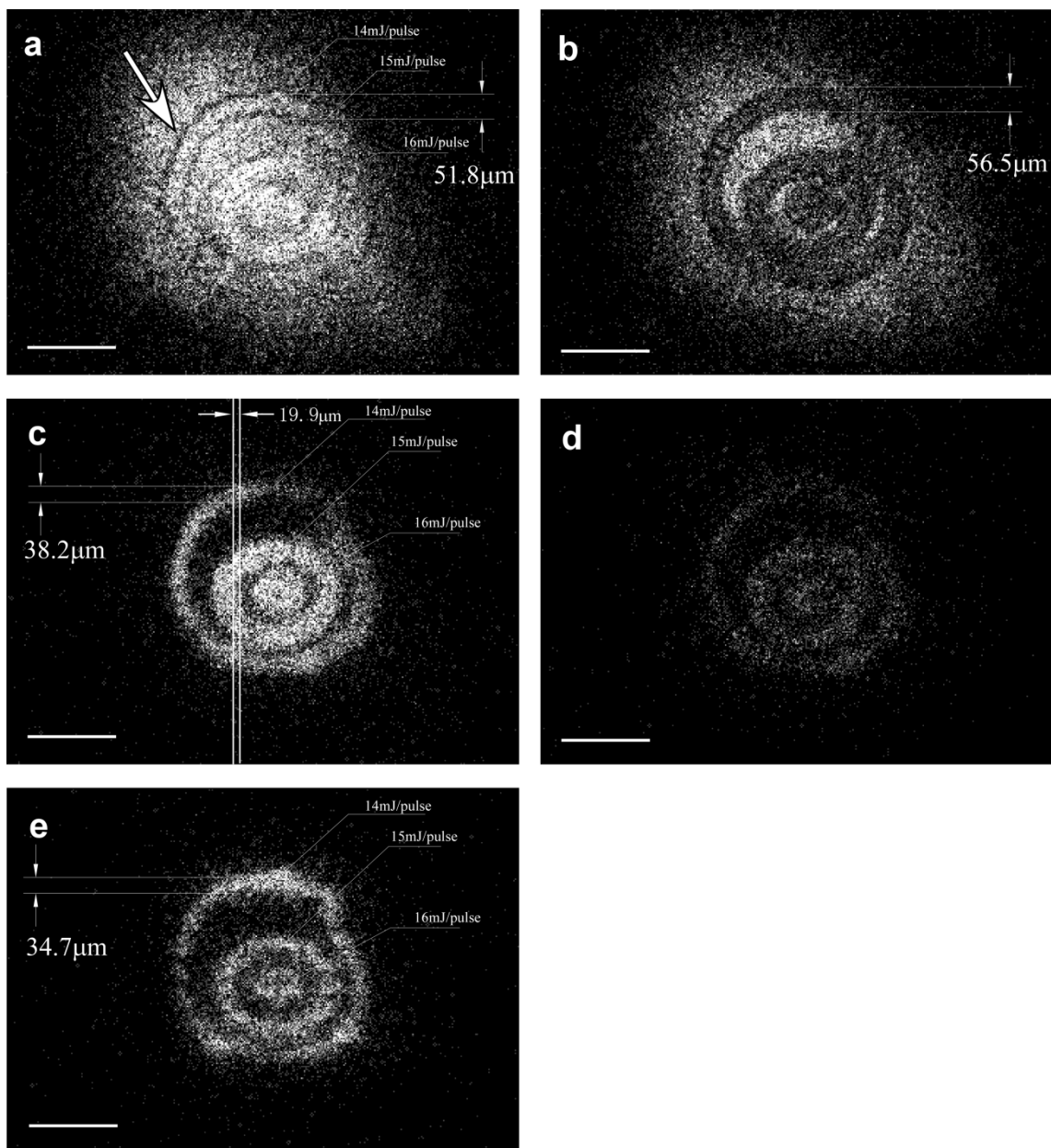


Figure 4